

Age-related changes in cerebellar and hypothalamic function accompany non-microglial immune gene expression, altered synapse organization, and excitatory amino acid neurotransmission deficits

Stephen J. Bonasera¹, Jyothi Arikath², Michael D. Boska³, Tammy R. Chaudoin¹, Nicholas W. DeKorver¹, Evan H. Goulding⁴, Traci A. Hoke¹, Vahid Mojtahedzadeh⁵, Crystal D. Reyelts¹, Balasrinivasa Sajja³, A. Katrin Schenk⁶, Laurence H. Tecott⁷, Tiffany A. Volden¹

¹Division of Geriatrics, University of Nebraska Medical Center, Durham Research Center II, Omaha, NE 68198, USA

²Monroe-Meyer Institute, University of Nebraska Medical Center, Durham Research Center II, Omaha, NE 68198, USA

³Department of Radiology, University of Nebraska Medical Center, College of Medicine, Omaha, NE 68198, USA

⁴Department of Psychiatry and Behavioral Sciences, Northwestern University, Chicago, IL 60611, USA

⁵The Institute for Addiction Sciences and Psychology (IRSA), Tehran, Iran

⁶Department of Physics, Randolph College, Lynchburg, VA 24503, USA

⁷Department of Psychiatry, University of California, San Francisco, San Francisco, CA, 94158, USA

Correspondence to: Stephen J. Bonasera; email: sbonasera@unmc.edu

Keywords: aging, pattern recognition receptor (PRR), hypothalamus, cerebellum, feeding, mouse physical activity, microarray

Received: June 08, 2016 **Accepted:** September 7 2016 **Published:** September 20, 2016

ABSTRACT

We describe age-related molecular and neuronal changes that disrupt mobility or energy balance based on brain region and genetic background. Compared to young mice, aged C57BL/6 mice exhibit marked locomotor (but not energy balance) impairments. In contrast, aged BALB mice exhibit marked energy balance (but not locomotor) impairments. Age-related changes in cerebellar or hypothalamic gene expression accompany these phenotypes. Aging evokes upregulation of immune pattern recognition receptors and cell adhesion molecules. However, these changes do not localize to microglia, the major CNS immunocyte. Consistent with a neuronal role, there is a marked age-related increase in excitatory synapses over the cerebellum and hypothalamus. Functional imaging of these regions is consistent with age-related synaptic impairments. These studies suggest that aging reactivates a developmental program employed during embryogenesis where immune molecules guide synapse formation and pruning. Renewed activity in this program may disrupt excitatory neurotransmission, causing significant behavioral deficits.

INTRODUCTION

Aging individuals vary in their susceptibility for developing mobility impairment or involuntary weight loss. For example, mobility impairments were noted in 36% of subjects enrolled in a large 6 year longitudinal trial studying adults 65+ years old who were functionally intact at enrollment [1]. Much of this loss

could not be attributed to sarcopenia, Parkinson's disease, or stroke. Similarly, about 15% of adults experience involuntary age-related weight loss in the absence of cancer, gastrointestinal disease, or stroke [2].

Weight loss and mobility declines are both harbingers of frailty, a clinical syndrome that increases the risk of functional loss and death [3]. Although etiologies of age-

related mobility and energy balance impairments are not well understood, there is good reason to suspect that changes in CNS structure and function may be involved. CNS aging alters brain anatomy [4,5]. Progressive loss or altered function of synapses in a specific CNS region ultimately impairs behaviors under that structure's control [6]. How aging changes synapse organization and overall synaptic activity, ultimately causing functional impairment, remains poorly understood. These questions have widespread societal impact, since considerable spending will be required in the coming decade to manage problems directly attributable to CNS aging.

We focused on determining the CNS processes underlying two clinically-significant phenotypes associated with aging: decreased physical activity and weight loss. We first demonstrate that different mouse strains have varying susceptibilities to age-related impairments in mobility and body weight. We then examine the regional impact of age-related changes in gene expression within the cerebellum and hypothalamus, two key regions that organize activity and energy-balance behaviors, and translate these findings to the human cerebellum. Finally, we studied the effect of these age-related changes in gene expression on synapse organization, and overall excitatory synaptic activity within these two CNS regions.

RESULTS

Aging mice have functional deficits

We began by examining how aging affected mouse functional status: food intake, water intake, and physical

activity. These behaviors were evaluated for 13-18 days in a custom-designed home cage behavioral monitoring (HCM) system following 5 days of acclimation [7]. We tested cohorts of young (2-3 mo), middle-aged (12-13 mo), and aged (21-24 mo) BALB and C57BL/6 mice. These two strains have distinct breeding lineages [8], and thus provide an indication of how genetic diversity might influence age-related CNS phenotypes. In C57BL/6 mice, locomotion (Figure 1, left panel) markedly decreased with age ($p < 0.011$, $F_{2,30} = 5.2$, one-way ANOVA), with a 32% difference noted between young and aged mice by *post hoc* testing ($p < 0.013$). By contrast, BALB mice demonstrated no age-related locomotor decreases. Furthermore, false discovery rate analysis (Supplemental Table 1A) showed that aged C57BL/6 mice were more likely to have mobility impairments when compared to either young C57BL/6 or aged BALB mice. For example, aged C57BL/6 mice had more impairments in locomotor-associated behaviors when compared to young C57BL/6 mice ($p < 0.042$, χ^2 test) or when compared to aged BALB mice ($p < 0.026$). Similarly, aged C57BL/6 mice had more impairments of nonlocomotor movement-associated behaviors when compared to young C57BL/6 mice ($p < 0.046$) or when compared to aged BALB mice ($p < 0.05$).

Further dissection of this mobility deficit revealed a significant decrease in the overall number of locomotor bouts occurring during the circadian dark cycle as well as decreased locomotor speed (Figure 2A). This decrease in locomotor bout frequency was incompletely compensated by an increase in locomotor bout duration (Figure 2B). Similar changes are observed across aging human cohorts [9]. Furthermore, locomotor paths of

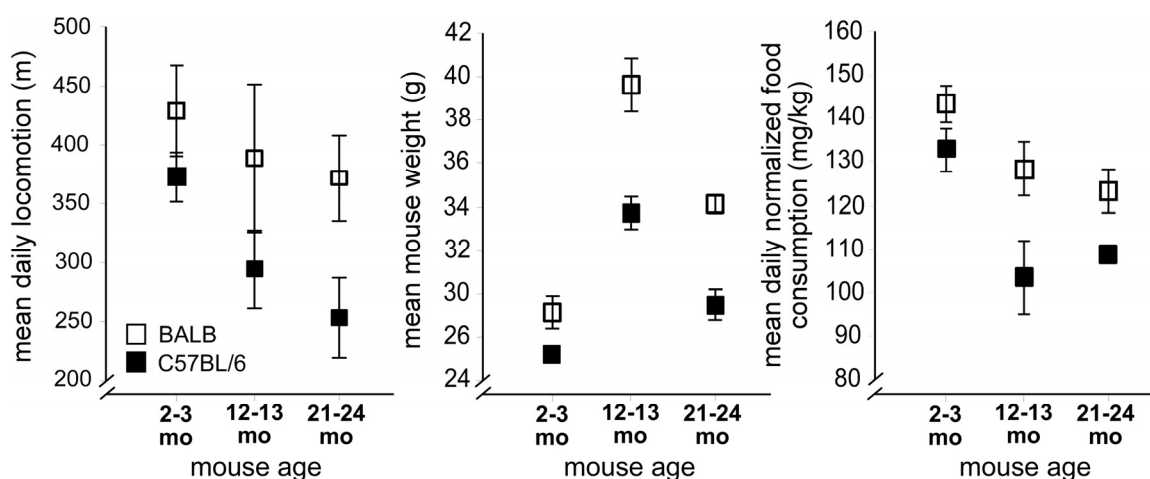


Figure 1. Strain-specific impairments in mouse mobility and energy balance occur with aging. Left: Decreased mean daily locomotion in aged C57BL/6 mice (filled rectangles), with preserved mean daily locomotion in aged BALB mice (open rectangles). Center: Body weight in aged C57BL/6 and BALB mice decreases between 12-13 months and 21-24 months. Right: Normalized food intake. For all figures, error bars are ± 1 standard error of the mean.

young C57BL/6 mice (Figure 2C) were significantly straighter ($p < 0.001$; across-mouse variability $p < 0.001$, within-mouse variability no effect) compared to locomotor paths of aged C57BL/6 mice, suggesting an age-related impact on cerebellar function (and related to tandem gait impairment commonly seen in older adults). By contrast, we observed no age-related difference in overall locomotion, locomotor bouts, or locomotor path straightness in BALB mice (Supplemental Figure 1A, B respectively, green traces).

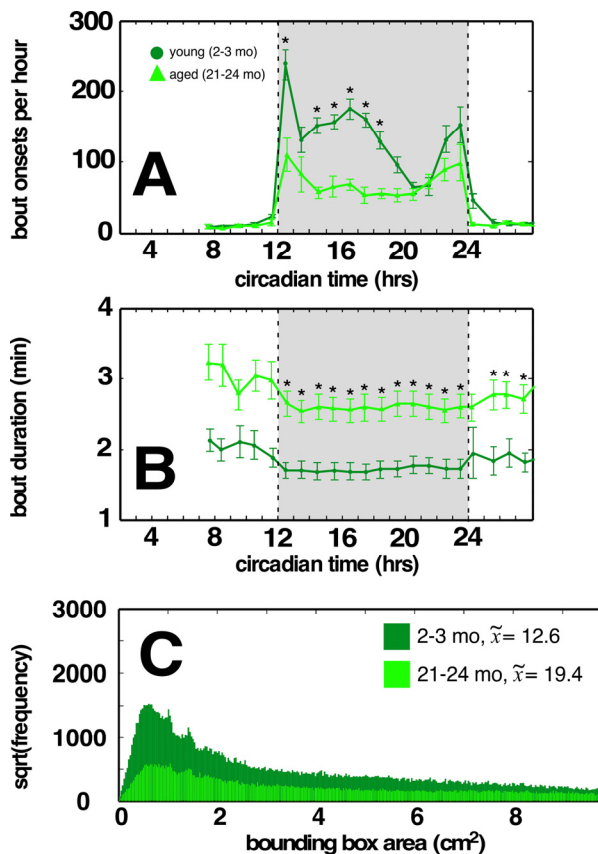


Figure 2. Aged C57BL/6 mice have fewer locomotor bouts during the dark cycle, and a greater proportion of weaving locomotor bouts compared to young cohorts. (A) Aged C57BL/6 mice display fewer bouts of dark cycle locomotion compared to young cohort. (B) Increased locomotor bout durations in aged C57BL/6 mice. (C) Distribution of minimum bounding rectangle areas (MBRs; cut off at 10 to better show small rectangle areas) for locomotor bouts of young and aged C57BL/6 mice. Smaller MBRs indicate more direct locomotor paths. Median values for each cohort in legend. Traces in light green correspond to aged mice, dark green correspond to young mice. Greyed region depicts dark cycle, dashed lines indicate dark cycle onset and offset, respectively. Asterisks indicate $p < 0.01$, Bonferroni corrected; error bars are \pm 1 standard error of the mean.

By contrast, aging BALB mice demonstrated dysregulated overall energy balance. Normal aging is characterized by body weight maintenance, and decreased basal metabolic rate, activity, and food consumption. Both BALB and C57BL/6 mice show significant weight loss between the middle-aged and aged cohorts (Figure 1, center panel, $p < 0.05$, $p < 0.0002$ respectively, one sided t-test). However, we found no significant differences between middle-aged and aged BALB mice in peak oxygen consumption ($\dot{V}O_2$), carbon dioxide production ($\dot{V}CO_2$), or adiposity (Supplemental Figure 2A). Aged BALB mice also maintain activity levels similar to those of young BALB mice, while aged C57BL/6 mice significantly decrease their activity. Furthermore, aged BALB mice tend to consume less chow (normalized to body weight) compared to middle-aged BALB mice, while aged C57BL/6 mice tend to consume more chow compared to middle-aged C57BL/6 mice (Figure 1, right panel). False discovery rate analysis further demonstrated that aged BALB mice showed impairments in more feeding-associated behaviors compared to aged C57BL/6 mice ($p < 0.036$; Supplemental Table 1B). Further analysis of energy balance dysregulation in aged BALB mice revealed a significant decrease in the overall number of circadian dark cycle feeding bouts and decreased bout food intake (Figure 3A). Again, this decrease in feeding bouts was incompletely compensated by an increase in feeding bout duration, leading to a 10-15% decrease in overall feeding in aged BALB mice (compared to young cohort, Figure 3B). In C57BL/6 mice, no age-related difference in overall food intake or feeding bouts was appreciated (Supplemental Figure 2B). Age-related changes in feeding patterns similar to aged BALB mice have also been reported in older human populations [10].

Altered CNS immune gene expression in aged mice

The molecular events underlying the above-described functional impairments remain poorly understood. To obtain an unbiased view of mRNA transcriptional changes associated with these behavioral deficits, we used whole mouse genome microarrays. Whole tissue cerebellar and hypothalamic mRNA expression was determined and compared between cohorts of young, middle-aged, and aged BALB and C57BL/6 mice (per Methods). Transcripts obtained originate from neuronal soma and dendrites, with minimal contribution from axonal projections [11]. Signal strength characteristics across all chips were similar, as were cross-sample correlations for each of the individual groups, suggesting good technical microarray performance (Supplemental Figure 3A-D for BALB hypothalamus,

BALB cerebellum, C57BL/6 hypothalamus, and C57BL/6 cerebellum, respectively).

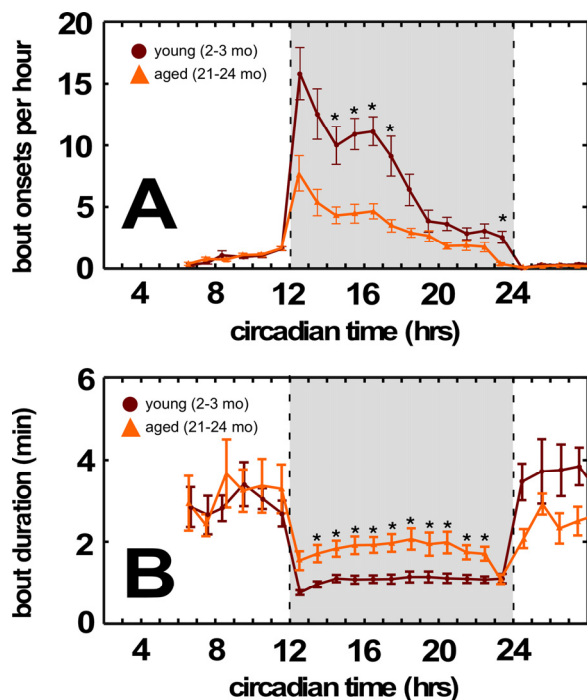


Figure 3. Aged BALB mice have fewer feeding bouts during the dark cycle. (A) Decreased feeding bouts in aged BALB mice. (B) Increased feeding bout duration in aged BALB mice. Traces in light orange correspond to young mice; traces in dark orange correspond to aged mice. Grayed region depicts dark cycle, dashed lines indicate dark cycle onset and offset, respectively. Asterisks indicate $p < 0.01$, Bonferroni corrected; error bars are ± 1 standard error of the mean.

Aging evokes modest changes in overall CNS gene expression (Figure 4, Venn diagram). Lists of genes differentially expressed between young and aged mice are provided in Supplemental Table 2 (BALB hypothalamus, BALB cerebellum, C57BL/6 hypothalamus, C57BL/6 cerebellum respectively). These changes occurred in both a strain- and site-specific manner (Figure 4 comparing BALB hypothalamus and C57BL/6 cerebellum; Supplemental Figure 4 comparing BALB cerebellum and C57BL/6 hypothalamus). In whole cerebellar and hypothalamic tissue of C57BL/6 and BALB mice, respectively, there was marked overexpression of transcripts characterized by ontology as having immune/defense function ($p < 0.001$ for both regions; Figure 4, also see Supplemental Table 2). Ontology analysis suggested that these transcripts belonged to specific functional categories, including classical major histocompatibility complex I (e.g. H2-D1, H2-K1), atypical major histocompatibility complex I (e.g. H2-Q1, H2-Q7), complement (e.g. C3, C1q,

C4b), cytokine/chemokine (e.g. Ccl6, Ccl12), pattern recognition receptors (e.g. Tlr2, Clec7a, Lgals3, Trem2, FcRs, Lilrb3), and cell adhesion molecules (e.g. Itgax, Lyz, Timp1). Predicted protein-protein interactions (STRING 9.1; string-db.org) further suggest that many genes overexpressed in the C57BL/6 cerebellum and BALB hypothalamus form membrane-bound signaling complexes (e.g. Fcgr3-Fcer1g-Tyrobp-Lilrb3-Ms4a6d-C1q; Clec7a-Tyrobp-Emr1-Ctss-Ly86-Igsf6-Mpeg1; Lgals3-Cd68-Capg-S100a4-Anxa4-Lgals3bp) that converge to activate NF κ B. RT-qPCR confirmed these age-related changes in gene expression for selected loci in whole hypothalamic tissue (Supplemental Figure 5). 16% of the cerebellar genes differentially expressed between young and old C57BL/6 mice are known NF κ B targets [12]; this value rises to 33% by including NF κ B target predictions by TRANSFAC (ver 7.0 Public 2005) [13]. Similarly, 10% of the hypothalamic genes differentially expressed between young and old BALB mice are known NF κ B targets, rising to 23% by including TRANSFAC predictions. Intriguingly, in human cerebellum we find age-related increases in expression of mRNAs homologous to those identified in the C57BL/6 mouse cerebellum (Figure 5). These changes occurred across all of the above categories, including MHC I molecules (HLA-B), complement (C3, C4b), PRRs (Lilrb3, Lgals3) and CAMs (Itgax, Spp1).

Immune genes do not localize to microglia

Age-related increases in the CNS expression of immune/defense related transcripts have been attributed to neuroinflammation [14-16]. If this were the case, then a majority of these changes should localize to microglia. Microglia are resident CNS mononuclear phagocytes, and account for the vast majority of CNS immunocytes. Furthermore, microglial activation is a key and necessary step supporting neuroinflammation. We used a multi-step magnetic bead based separation process combined with molecular and functional validations [17] to obtain highly enriched populations (65-90% CD11b(+) total cells within suspension) of both parenchymal and perivascular microglia from the cerebellum and hypothalamus of young, middle-aged, and aged BALB and C57BL/6 mice. RT-qPCR gene expression assays found that these microglia clearly did not contribute to most of the observed age-related changes in whole tissue gene expression (Figure 6). Microglia only contributed to the age-associated C3 increase in the C57BL/6 cerebellum (Figure 6A). In the BALB hypothalamus (Figure 6B), expression of C1q and Lilrb3 were decreased in microglia derived from aged mice ($p < 0.01$). These results strongly suggest that most of the age-related changes in cerebellar and hypothalamic immune/defense gene expression do not localize to CNS microglia.

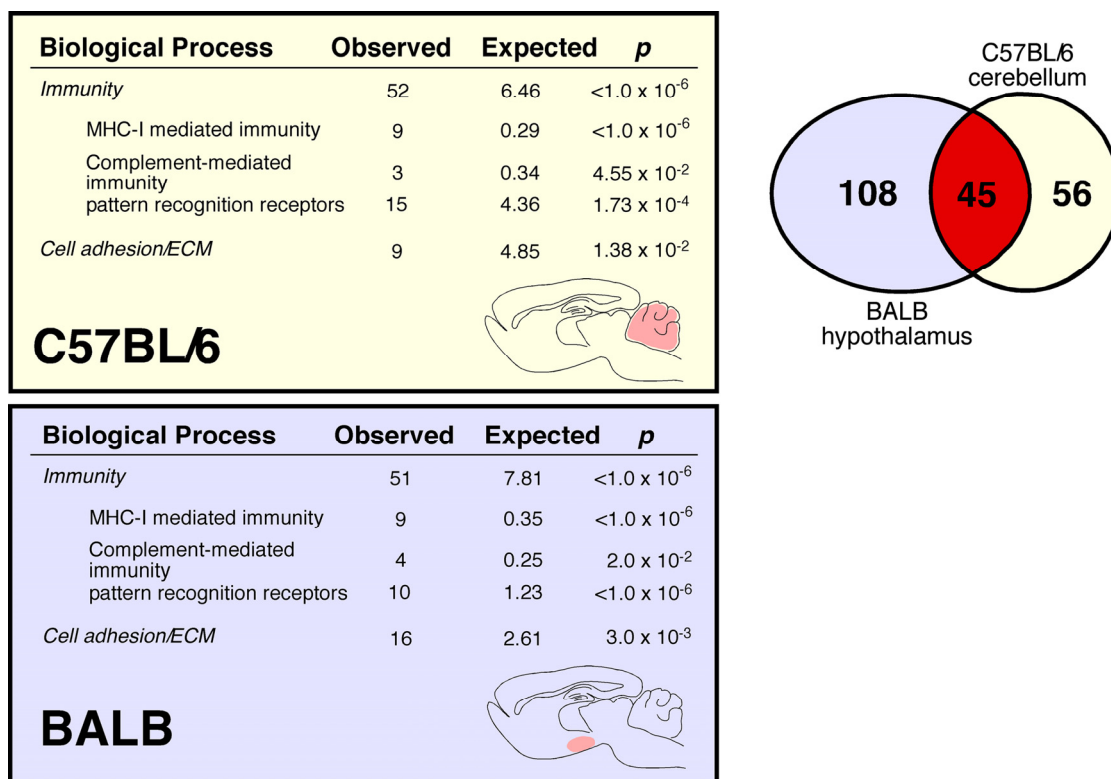


Figure 4. Age-associated increase in C57BL/6 cerebellar and BALB hypothalamic expression of immune transcripts. Venn diagram demonstrates that although these two regions have different cellular architectures and functions, they share considerable overlap in age-related changes in gene expression. In male C57BL/6 cerebellum, we identify 101 differentially expressed genes (DEGs), 100 upregulated in aged mice. In male BALB hypothalamus, we identify 153 DEGs, 113 upregulated in aged mice. Of note, 45 of these genes are differentially expressed in both C57BL/6 cerebellum and BALB hypothalamus; the probability of this occurring by chance is $p < 0.0001$. We measured gene expression with Agilent Whole Mouse Genome 4x44k arrays that use 60-mer probes to detect 41,174 full length mouse genes and ESTs. Following array quality control and normalization, we identified differentially expressed genes by log posterior odds (B) values > 0 (Supplemental Methods).

Synapse changes accompany altered PRR expression

In this light it is interesting to note that recent studies have found that pattern recognition molecules play an important role during both synaptogenesis and synaptic pruning phases of CNS development [18]. In the developing mouse thalamus, MHC Class I molecules demonstrate an activity-dependent expression pattern [19], and loss of these molecules leads to decreased synaptic pruning [20] and altered visual cortex plasticity [21]. Similar disruptions of synaptic pruning or plasticity are observed with loss of Clq (in the thalamus), PirB (in the primary visual cortex), and H2-K^b/H2-D^b (in the cerebellar Purkinje layer) [22-24]. MHC Class I molecules also regulate hippocampal synaptic activity [25]. We thus tested the hypothesis that increased expression of these PRR transcripts was associated with altered excitatory synapse organization. Given our earlier findings, we predicted that age-related synaptic changes should be more pronounced in the

cerebellum of C57BL/6 mice compared with BALB mice, and in the hypothalamus of BALB mice compared with C57BL/6 mice. To measure synaptic counts in these regions at highest accuracy, we employed a modified array tomography protocol. Ultrathin (90 nm) sections were prepared from the cerebellum of BALB and C57BL/6 mice from young and aged cohorts; thin (10 μ m) sections were prepared from the hypothalamus of BALB and C57BL/6 mice from young and aged cohorts (Supplemental Methods). Cell nuclei were visualized with DAPI, and excitatory synapses were visualized with antibodies directed against Vglut1. We chose C3 as a molecule increased in expression in both BALB hypothalamus and C57BL/6 cerebellum. Figure 7A shows representative photomicrographs in young and old C57BL/6 cerebellum, as well as quantified puncta counts (quantification workflow provided in Supplemental Figure 6); Figure 7B shows the equivalent figure for the young and old BALB hypothalamic arcuate nucleus.

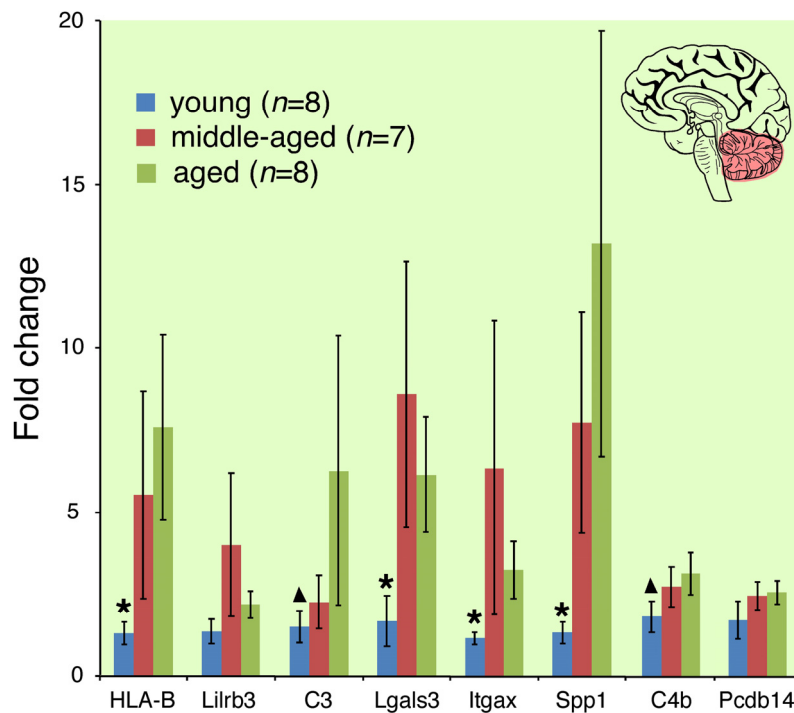


Figure 5. Cerebellar immune transcript expression increases with age in community-dwelling adults. Asterisk indicates gene expression in young cohort significantly different from middle-aged and aged cohorts ($p < 0.05$); triangle indicates gene expression in young cohort significantly different from aged cohort. Analogous genes were differentially expressed in the cerebellum of aged C57BL/6 mice with motor deficits.

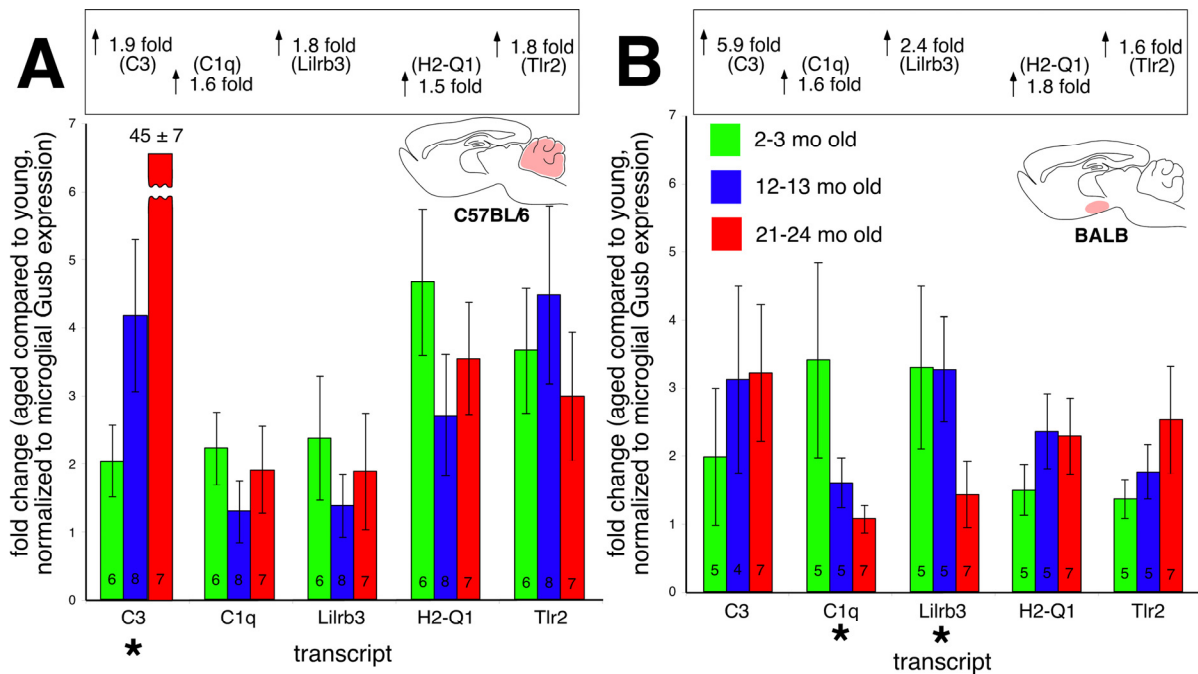


Figure 6. Microglial-specific expression of immune transcripts found upregulated with age in whole tissue (A) C57BL/6 cerebellum and (B) BALB hypothalamus. Values in each bar depict number of biological replicates. With the exception of C3 expression in the C57BL/6 cerebellum, no transcripts increase microglial expression with age. Values in the boxes above each graph show overall changes in transcript expression from whole tissue RT-qPCR experiments.

In the cerebellar internal granule cell layer, we observe a marked age-associated increase in both Vglut1 and C3 expression in C57BL/6, but not BALB, mice (Figure 7A; 2-way ANOVA with mouse strain and age as pri-

mary factors; strain \times age interaction $p < 0.04$ for Vglut1; $p < 0.001$ for C3). Specifically, in C57BL/6 mice, internal granule cell layer Vglut1 expression increases nearly 20% with age; in BALB mice, Vglut1 baseline

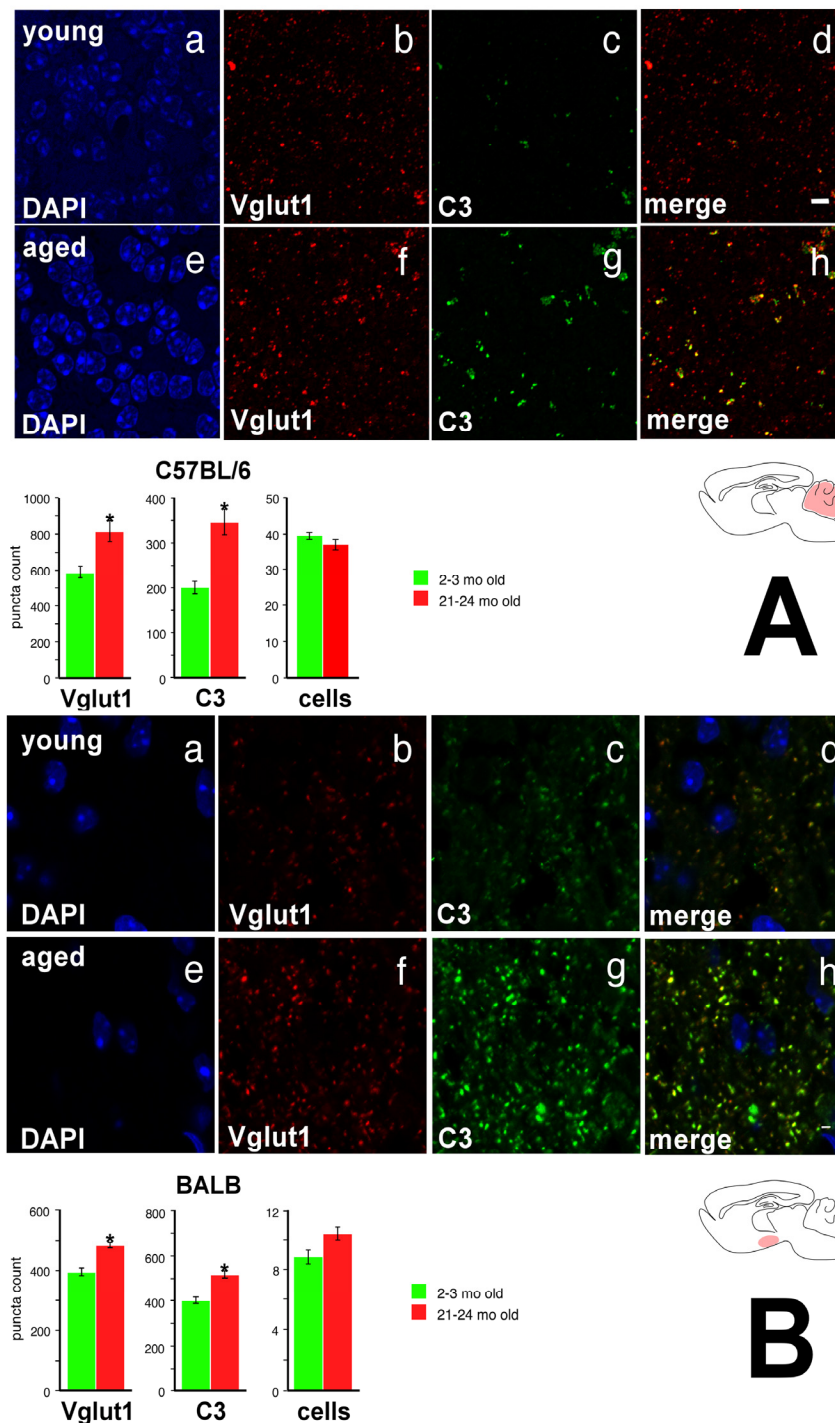


Figure 7. Vglut1 and C3 show increased expression in the cerebellar internal granule cell layer of the aged C57BL/6 mouse and in the hypothalamic arcuate nucleus of the aged BALB mouse. (A) C57BL/6 cerebellar internal granule cell layer. **a** DAPI stain, young. **b** Vglut1 immunoreactivity, young. **c** C3 immunoreactivity, young. **d** Merge, young. Note significant colocalization of Vglut1 and C3 staining, particularly for more intense puncta. **e** DAPI, aged. **f** Vglut1, aged. **g** C3, aged. **h** Merge, aged. Bottom: Quantification of Vglut1, C3, and DAPI. (B) BALB hypothalamic arcuate nucleus. Panels **a-h** as above. Again, note significant colocalization of Vglut1 and C3 staining, particularly for more intense puncta. Asterisk denotes $p < 0.01$. Scale bar 4 μ m.

expression is lower in young mice, and does not significantly change with age. We did not find any size difference in counted puncta. No significant differences were appreciated in either Vglut1 or C3 expression in aged BALB mice compared to young BALB counterparts (Supplemental Figure 7A). There were no age-related differences noted in overall cell count in either C57BL/6 or BALB mice, making neurodegeneration an unlikely explanation for this phenotype.

We further note that in the hypothalamic arcuate nucleus, we observe a marked age-associated increase in both Vglut1 and C3 expression in BALB (Figure 7B), but not C57BL/6 (Supplemental Figure 7B), mice (2-way ANOVA with mouse strain and age as primary factors; strain \times age interaction $p < 0.001$ for Vglut1; $p < 0.007$ for C3). While young BALB and C57BL/6 mice both show the same degree of Vglut1 expression, with aging we find a nearly 20% increase in BALB arcuate Vglut1 expression that is not seen in the aged C57BL/6 mouse. Again, no size difference was noted in

counted puncta, and there were no age-related differences in arcuate hypothalamus cell counts. These findings suggest that aging increases the number of excitatory synapse components in CNS regions where we observe increased expression of immune, complement, and pattern recognition genes with age, but does not change excitatory synapse organization in CNS regions where these age-related patterns of gene expression do not occur.

Functional impairment in aged synapses

To determine if the increased synapse counts observed in the aged C57BL/6 cerebellum and aged BALB hypothalamus were associated with a functional outcome, we assessed excitatory amino acid activity across the entire cerebellar internal granule cell layer and hypothalamus using manganese-enhanced MRI (MEMRI, supplemental methods). Neuronal Mn^{++} transport occurs in an activity-dependent manner analogous to calcium; however, Mn^{++} is paramagnetic,

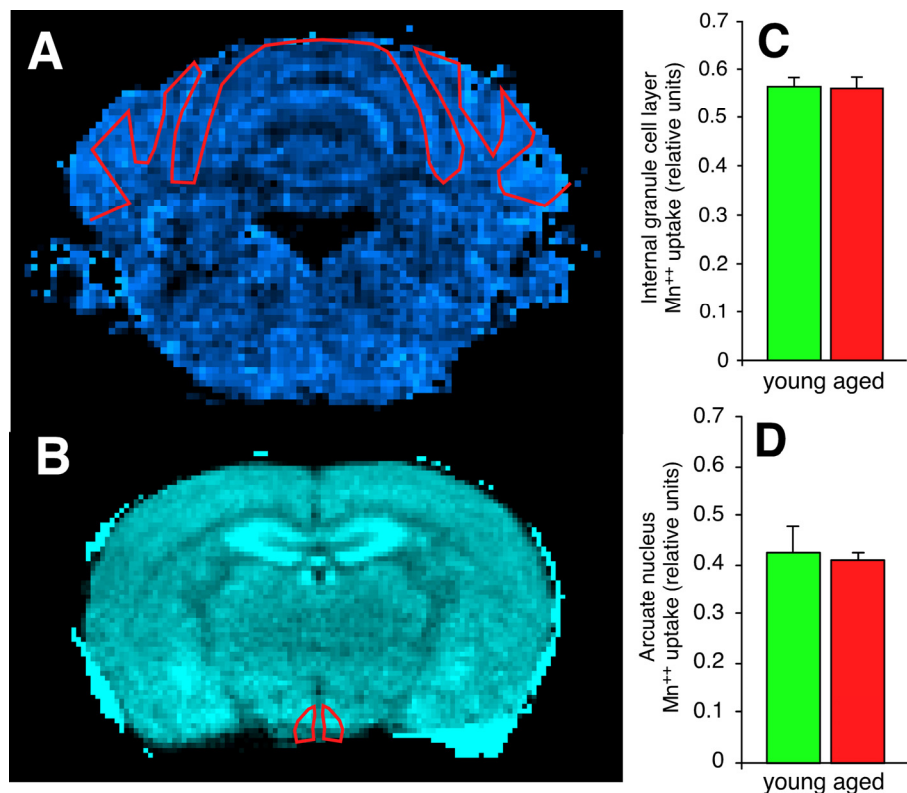


Figure 8. Synapses in the cerebellar internal granule cell layer of the aged C57BL/6 mouse and in the hypothalamic arcuate nucleus of the aged BALB mouse have functional deficits in excitatory amino acid neurotransmission. (A) Scaled difference MRI image of mouse cerebellum at approximately bregma -6.96 mm. Regions with higher Ca^{++} uptake are brighter on this colormap. The red line depicts the region-of-interest (ROI) drawn to include the internal granule cell layer. **(B)** Scaled difference MRI image of mouse hypothalamus at approximately bregma -1.46 mm. **(C, D)** Despite both regions demonstrating increased expression of regional-appropriate vesicular glutamate transporters, there is no evidence of increased post-synaptic Ca^{++} uptake in either the cerebellar internal granule cell layer **(C)** or the hypothalamic arcuate nucleus **(D)**.

causing reduction of T_1 in proportion to concentration, which can be measured using T_1 weighted imaging. Thus, Mn^{++} enhances MRI tissue signals in direct proportion to overall excitatory amino acid activity. Our results show no age-related increase in either C57BL/6 cerebellar internal granule cell layer (Figure 8A,C) or BALB hypothalamic arcuate nucleus (Figure 8B,D) excitatory amino acid activity. These findings do not rule out the possibility of increased excitatory amino acid activity below the MEMRI detection threshold in aged compared to young mice; however, changes of this magnitude are below expected biological signaling thresholds, and would require electrophysiology to verify. To rule out the possibility that age-related vascular disease contributed to our phenotypes, we further evaluated diffusion tensor images for all subjects. There were no significant age-related changes in water diffusion characteristics or vascular disease in either C57BL/6 or BALB mice (Supplemental Figure 8). These findings support the conclusion that the increased number of excitatory synapses present in the aged C57BL/6 cerebellar internal granule cell layer and aged BALB arcuate hypothalamic nucleus have a currently uncharacterized functional deficit.

DISCUSSION

In summary, we have framed a new model that further clarifies how cerebellar and hypothalamic aging cause mobility and energy balance impairments in aging mice. We demonstrate patterns of dysregulated CNS function associated with age-related behavioral phenotypes at molecular, cellular, and organ scales of organization. We further show that these patterns of dysregulated function have strong genetic predispositions, with some mouse strains developing specific age-related impairments in mobility or feeding, while other mouse strains do not. Analogous situations are observed in human aging [26, 27]. We show that aging reactivates CNS regional expression of classical and atypical MHC-1, complement, PRRs, and CAMs in a nonmicroglial context. Similar findings have been observed regarding C1q, whose expression increases in the aging mouse hippocampus and is accompanied by synaptic and behavioral impairments [28]. We also observe increased cerebellar expression of homologous transcripts in older human subjects. At a synaptic level of organization, we observe more excitatory presynaptic puncta in CNS regions where age-associated increases in immune gene expression occur. Similar age-related synapse dynamics have been noted in primary sensorimotor cortex of aged mice [29]. This increased number of excitatory synaptic components in both the aged cerebellum and hypothalamus did not evoke increased postsynaptic Ca^{++} , suggesting an age-

associated synaptic defect. This defect may arise from either altered presynaptic vesicular glutamate content [30, 31], decreased synaptic vesicle exocytosis probability [32, 33], or attenuated postsynaptic Ca^{++} signaling (multiple potential mechanisms affecting AMPAR trafficking and postsynaptic persistence). Ultimately, these deficits lead to impaired cerebellar function in C57BL/6 mice (demonstrated by their age-associated ataxia and locomotor loss) and impaired hypothalamic function in BALB mice (demonstrated by decreased food consumption in aged compared to middle-aged mice). Age-related losses in mobility and energy balance prominently affect substantial populations of older men and women, increasing health care utilization and costs while worsening personal quality of life. The concept that developmental programs active during embryogenesis, silent in adulthood, and reactivated with advancing age could lead to functional deficits is novel, and may be relevant to other organ systems.

We propose that age-related functional deficits arise through the following sequence. First, damage-associated molecular patterns (DAMPs) within the CNS matrix activate a multiplicity of neuronal PRRs, including C3R, C1qR, Trem2, Fcrlg, Fcgr2b, Fcgr3, Clec7a, Lgals3, Lilrb3, and so on. We suspect that signaling from these sources stimulates NF κ B activity *in vivo*; for example, mice with mutations delaying I κ B α (NF κ B primary functional inhibitor) synthesis show increased NF κ B activity after excitatory neuronal stimuli, and developed more excitatory synapses in *in vitro* neuronal culture [34]. Most of the PRRs we identified signal through pathways that drive NF κ B activation [35-37]. Furthermore, many of the genes we identified as differentially expressed with aging and associated with functional impairments are demonstrated NF κ B targets [12, 13]. Under baseline conditions, NF κ B is known to regulate neuronal responses to excitatory neurotransmission [38-40], including induction of BDNF [41], Grm2 [42], Grin2A [43], and Grin [44]. PRR signaling thus confounds neuronal NF κ B signaling evoked by AMPAR/NMDAR activity, falsely indicating increased excitatory neuronal activity. Increased transcription at NF κ B loci alters coordinated expression of excitatory synapse components, leading to imbalances in proteins required to assemble excitatory synapses and the creation of excitatory synapses with functional impairments. These synapses, as well as excess protein trafficked to the synapse, in turn undergo accelerated turnover, thus increasing matrix DAMP concentrations [45]. Continued activity of this positive feedback loop ultimately degrades hypothalamic and cerebellar synaptic organization, leading to functional loss. In

support of this concept, interventions inhibiting hypothalamic IKK β or NF κ B activity in aged animals ameliorate age-related feeding phenotypes [46].

METHODS

Young (Y, 2-3 mo), middle-aged (M, 12-13 mo), and aged (A, 21-24 mo) male C57BL/6 and BALB mice were obtained from the NIA aged rodent colony; human tissue gifts were obtained from the UNMC brain bank. Mouse behavioral studies were performed per [7]. Subject numbers for presented figures: BALB (Y $n=10$, M $n=7$, A $n=11$), C57BL/6 (Y $n=10$, M $n=9$, A $n=11$). Behavioral studies were replicated in at least two separate cohorts. Whole tissue hypothalamic and cerebellar RNA was purified by standard methods, assessed for degradation, and hybridized to Agilent 4x44k Whole Mouse Genome microarrays per manufacturer protocol. Array data analysis included quantile normalization, determination of differential gene expression, and classification of differential gene expression by ontology-based methods. Subject numbers for microarray studies were as follows: BALB hypothalamus (Y $n=7$, M $n=5$, A $n=6$); C57BL/6 cerebellum (Y $n=4$, M $n=2$, A $n=6$). Microglial studies were performed as described by [15]. Subject numbers were as follows: BALB hypothalamus (Y $n=6$, M $n=8$, A $n=7$); C57BL/6 cerebellum (Y $n=5$, M $n=5$, A $n=7$). For studies examining hypothalamic and cerebellar synapse organization, mice were sacrificed either by rapid decapitation (for cerebellar studies) or intracardiac perfusion (hypothalamic studies). Thin sections (90 nm cerebellum, 10 μ m hypothalamus) were prepared and stained for nuclei, C3, and Vglut1. Multiple windows were visualized within the cerebellar internal granule cell layer and hypothalamic arcuate nucleus; cell counts were quantified by ImageJ and analyzed by ANOVA. Subject numbers were as follows: BALB hypothalamus (Y $n=7$, A $n=7$); C57BL/6 hypothalamus (Y $n=4$, A $n=5$); BALB cerebellum (Y $n=3$, A $n=4$); C57BL/6 cerebellum (Y $n=4$, A $n=4$). Mn⁺⁺ enhanced MRI was performed per [47]. Subject numbers were as follows: BALB (Y $n=5$, A $n=4$); C57BL/6 (Y $n=5$, A $n=5$).

More Methods, MiQE, GEO archive accession number, UNMC digital link to the raw behavioral data could be found in Supplemental Material.

ACKNOWLEDGEMENTS

The authors thank the Functional Genomics Core (UCSF Sandler Center for Basic Research in Asthma; A. Barczak, R. Barbeau, W. Xu, C. Eisner, D. Earle), Genome Analysis Core Facility (UCSF Helen Diller

Family Comprehensive Cancer Center; K. Copren), Genomics Core (Gladstone Institutes; L. Ta), Flow Cytometry Core (Gladstone Institutes; V. Stepps, M. Bigos), UNMC Cell Analysis Facility (M.L. Michalak, V.B. Smith, C.A. Kuszynski), UNMC Small Animal Imaging Laboratory (Y. Liu, M. Uberti, M. Melton, B. Berrigan, E. McIntyre), UNMC Brain Bank (S.A. Kazmi), UNMC Electron Microscopy Core (T. Barger), UNMC Tissue Science Facility (D. Wert), and UNMC Confocal Laser Scanning Microscope Core for their technical expertise and skills. We thank Charles McCulloch, Ph.D. (UCSF), for discussions regarding analysis of behavioral data, and Adams Kusi Appiah (UNMC) for R expertise. We thank Leo Arellanos, Karl Huebner, Rachel Tecott, and Chris Dinh for their assistance in performing microarray and home cage monitoring experiments. We thank Ross Henderson (DiLog Instruments), Lance C. Pérez, Ph.D., Jay Carlson, M.S.EE, and Steven Parkison, B.S.EE (University of Nebraska, Lincoln) for their discussions regarding the mouse home cage monitoring system. We thank Anna Dunaevsky, Ph.D. and Louis Ptáček, M.D., Ph.D. for their comments on this manuscript.

AUTHOR CONTRIBUTIONS

All studies conceived, performed, analyzed, reported by SJB. JA, TAH, NWD assisted, performed, and analyzed all immunochemical studies. TRC, CDR, BS, MDB assisted, performed, and analyzed all neuroimaging studies. VM, TAH, CDR, TAV assisted and performed gene expression, RT-qPCR, and microglial studies. TRC, VM, NWD performed mouse behavioral studies; AKS and EHG assisted in their planning and analysis. EHG and LHT assisted in study conception and manuscript preparation.

FUNDING

This study was supported by NIH grant R01-AG031158 and startup funds from the University of Nebraska Medical Center. Finally, we thank Jane F. Potter, M.D., and the members of the UNMC Division of Geriatrics for their support.

CONFLICTS OF INTEREST

LHT is a founder, EthoMetrics Inc. SJB, JA, NWD, AKS, EHG, TAH, TRC, BS, MDB, CDR, TAV, VM have no conflicts of interest.

REFERENCES

1. Guralnik JM, LaCroix AZ, Abbott RD, Berkman LF, Satterfield S, Evans DA, Wallace RB. Maintaining

- mobility in late life. I. Demographic characteristics and chronic conditions. *Am J Epidemiol.* 1993; 137:845–57.
2. Hays NP, Roberts SB. The anorexia of aging in humans *Physiol Behav.* 2006; 88:257–66. doi.org/10.1016/j.physbeh.2006.05.029
3. Kulmala J, Nykänen I, Hartikainen S. Frailty as a predictor of all-cause mortality in older men and women. *Geriatr Gerontol Int.* 2014; 14:899–905. doi.org/10.1111/ggi.12190
4. Matsumoto A, Okada R, Arai Y. Synaptic changes in the hypothalamic arcuate nucleus of old male rats. *Exp Neurol.* 1982; 78:583–90. doi.org/10.1016/0014-4886(82)90076-0
5. Zhang C, Zhu Q, Hua T. Effects of aging on dendritic arborizations, dendritic spines, and somatic configurations of cerebellar Purkinje cells of old cat. *Pak J Zool.* 2011; 43:1191–96.
6. Poe GR, Teed RG, Insel N, White R, McNaughton BL, Barnes CA. Partial hippocampal inactivation: effects on spatial memory performance in aged and young rats. *Behav Neurosci.* 2000; 114:940–49. doi.org/10.1037/0735-7044.114.5.940
7. Goulding EH, Schenk AK, Juneja P, MacKay AW, Wade JM, Tecott LH. A robust automated system elucidates mouse home cage behavioral structure. *Proc Natl Acad Sci USA.* 2008; 105:20575–82. doi.org/10.1073/pnas.0809053106
8. Petkov PM, Ding Y, Cassell MA, Zhang W, Wagner G, Sargent EE, Asquith S, Crew V, Johnson KA, Robinson P, Scott VE, Wiles MV. An efficient SNP system for mouse genome scanning and elucidating strain relationships. *Genome Res.* 2004; 14:1806–11. doi.org/10.1101/gr.2825804
9. Schimpl M, Moore C, Lederer C, Neuhaus A, Sambrook J, Danesh J, Ouwehand W, Daumer M. Association between walking speed and age in healthy, free-living individuals using mobile accelerometry—a cross-sectional study. *PLoS One.* 2011; 6:e23299. doi.org/10.1371/journal.pone.0023299
10. Howarth NC, Huang TT, Roberts SB, Lin B-H, McCrory MA. Eating patterns and dietary composition in relation to BMI in younger and older adults. *Int J Obes.* 2007; 31:675–84.
11. Holt CE, Schuman EM. The central dogma decentralized: new perspectives on RNA function and local translation in neurons. *Neuron.* 2013; 80:648–57. doi.org/10.1016/j.neuron.2013.10.036
12. Boston University (US). NF- κ B Target Genes. Thomas Gilmore, Ph.D., Biology Department, Boston University, 5 Cummington Mall, Boston MA. 2016. www.bu.edu/nf-kb/gene-resources/target-genes
13. Matys V, Fricke E, Geffers R, Gössling E, Haubrock M, Hehl R, Hornischer K, Karas D, Kel AE, Kel-Margoulis OV, Kloos DU, Land S, Lewicki-Potapov B, et al. TRANSFAC: transcriptional regulation, from patterns to profiles. *Nucleic Acids Res.* 2003; 31:374–78. doi.org/10.1093/nar/gkg108
14. Lee CK, Klopp RG, Weindrich R, Prolla TA. Gene expression profile of aging and its retardation by caloric restriction. *Science.* 1999; 285:1390–93. doi.org/10.1126/science.285.5432.1390
15. Prolla TA. DNA microarray analysis of the aging brain. *Chem Senses.* 2002; 27:299–306. doi.org/10.1093/chemse/27.3.299
16. Jiang CH, Tsien JZ, Schultz PG, Hu Y. The effects of aging on gene expression in the hypothalamus and cortex of mice. *Proc Natl Acad Sci USA.* 2001; 98:1930–34. doi.org/10.1073/pnas.98.4.1930
17. Volden TA, Reyelts CD, Hoke TA, Arikath J, Bonasera SJ. Validation of flow cytometry and magnetic bead-based methods to enrich CNS single cell suspensions for quiescent microglia. *J Neuroimmune Pharmacol.* 2015; 10:655–65. doi.org/10.1007/s11481-015-9628-7
18. Needleman LA, Liu XB, El-Sabeawy F, Jones EG, McAllister AK. MHC class I molecules are present both pre- and postsynaptically in the visual cortex during postnatal development and in adulthood. *Proc Natl Acad Sci USA.* 2010; 107:16999–7004. doi.org/10.1073/pnas.1006087107
19. Corriveau RA, Huh GS, Shatz CJ. Regulation of class I MHC gene expression in the developing and mature CNS by neural activity. *Neuron.* 1998; 21:505–20. doi.org/10.1016/S0896-6273(00)80562-0
20. Huh GS, Boulanger LM, Du H, Riquelme PA, Brotz TM, Shatz CJ. Functional requirement for class I MHC in CNS development and plasticity. *Science.* 2000; 290:2155–59. doi.org/10.1126/science.290.5499.2155
21. Datwani A, McConnell MJ, Kanold PO, Micheva KD, Busse B, Shamloo M, Smith SJ, Shatz CJ. Classical MHCI molecules regulate retinogeniculate refinement and limit ocular dominance plasticity. *Neuron.* 2009; 64:463–70. doi.org/10.1016/j.neuron.2009.10.015
22. Stevens B, Allen NJ, Vazquez LE, Howell GR, Christopherson KS, Nouri N, Micheva KD, Mehalow AK, Huberman AD, Stafford B, Sher A, Litke AM, Lamb-

- ris JD, et al. The classical complement cascade mediates CNS synapse elimination. *Cell*. 2007; 131:1164–78. doi.org/10.1016/j.cell.2007.10.036
23. Syken J, Grandpre T, Kanold PO, Shatz CJ. PirB restricts ocular-dominance plasticity in visual cortex. *Science*. 2006; 313:1795–800. doi.org/10.1126/science.1128232
24. McConnell MJ, Huang YH, Datwani A, Shatz CJ. H2-K(b) and H2-D(b) regulate cerebellar long-term depression and limit motor learning. *Proc Natl Acad Sci USA*. 2009; 106:6784–89. doi.org/10.1073/pnas.0902018106
25. Goddard CA, Butts DA, Shatz CJ. Regulation of CNS synapses by neuronal MHC class I. *Proc Natl Acad Sci USA*. 2007; 104:6828–33. doi.org/10.1073/pnas.0702023104
26. Karasik D, Hannan MT, Cupples LA, Felson DT, Kiel DP. Genetic contribution to biological aging: the Framingham Study. *J Gerontol A Biol Sci Med Sci*. 2004; 59:218–26. doi.org/10.1093/gerona/59.3.B218
27. Gurland BJ, Page WF, Plassman BL. A twin study of the genetic contribution to age-related functional impairment. *J Gerontol A Biol Sci Med Sci*. 2004; 59:859–63. doi.org/10.1093/gerona/59.8.M859
28. Stephan AH, Madison DV, Mateos JM, Fraser DA, Lovelett EA, Coutellier L, Kim L, Tsai HH, Huang EJ, Rowitch DH, Berns DS, Tenner AJ, Shamloo M, Barres BA. A dramatic increase of C1q protein in the CNS during normal aging. *J Neurosci*. 2013; 33:13460–74. doi.org/10.1523/JNEUROSCI.1333-13.2013
29. Mostany R, Anstey JE, Crump KL, Maco B, Knott G, Portera-Cailliau C. Altered synaptic dynamics during normal brain aging. *J Neurosci*. 2013; 33:4094–104. doi.org/10.1523/JNEUROSCI.4825-12.2013
30. Wilson NR, Kang J, Hueske EV, Leung T, Varoqui H, Murnick JG, Erickson JD, Liu G. Presynaptic regulation of quantal size by the vesicular glutamate transporter VGLUT1. *J Neurosci*. 2005; 25:6221–34. doi.org/10.1523/JNEUROSCI.3003-04.2005
31. Wojcik SM, Rhee JS, Herzog E, Sigler A, Jahn R, Takamori S, Brose N, Rosenmund C. An essential role for vesicular glutamate transporter 1 (VGLUT1) in postnatal development and control of quantal size. *Proc Natl Acad Sci USA*. 2004; 101:7158–63. doi.org/10.1073/pnas.0401764101
32. Fremeau RT Jr, Troyer MD, Pahner I, Nygaard GO, Tran CH, Reimer RJ, Bellocchio EE, Fortin D, Storm-Mathisen J, Edwards RH. The expression of vesicular glutamate transporters defines two classes of excitatory synapse. *Neuron*. 2001; 31:247–60. doi.org/10.1016/S0896-6273(01)00344-0
33. Varoqui H, Schäfer MK, Zhu H, Weihe E, Erickson JD. Identification of the differentiation-associated Na⁺/PI transporter as a novel vesicular glutamate transporter expressed in a distinct set of glutamatergic synapses. *J Neurosci*. 2002; 22:142–55.
34. Shim DJ, Yang L, Reed JG, Noebels JL, Chiao PJ, Zheng H. Disruption of the NF- κ B /I κ B α autoinhibitory loop improves cognitive performance and promotes hyperexcitability of hippocampal neurons. *Mol Neurodegener*. 2011; 6:42–56. doi.org/10.1186/1750-1326-6-42
35. Mócsai A, Ruland J, Tybulewicz VL. The SYK tyrosine kinase: a crucial player in diverse biological functions. *Nat Rev Immunol*. 2010; 10:387–402. doi.org/10.1038/nri2765
36. Kaltschmidt B, Widera D, Kaltschmidt C. Signaling via NF-kappaB in the nervous system. *Biochim Biophys Acta*. 2005; 1745:287–99. doi.org/10.1016/j.bbamcr.2005.05.009
37. Sun S-C. The noncanonical NF- κ B pathway. *Immunol Rev*. 2012; 246:125–40. doi.org/10.1111/j.1600-065X.2011.01088.x
38. Meberg PJ, Kinney WR, Valcourt EG, Routtenberg A. Gene expression of the transcription factor NF- κ B in hippocampus: regulation by synaptic activity. *Brain Res Mol Brain Res*. 1996; 38:179–90. doi.org/10.1016/0169-328X(95)00229-L
39. Meffert MK, Chang JM, Wiltgen BJ, Fanselow MS, Baltimore D. NF- κ B functions in synaptic signaling and behavior. *Nat Neurosci*. 2003; 6:1072–78. doi.org/10.1038/nn1110
40. Boersma MC, Dresselhaus EC, De Biase LM, Mihalas AB, Bergles DE, Meffert MK. A requirement for nuclear factor-kappaB in developmental and plasticity-associated synaptogenesis. *J Neurosci*. 2011; 31:5414–25. doi.org/10.1523/JNEUROSCI.2456-10.2011
41. Saha RN, Liu X, Pahan K. Up-regulation of BDNF in astrocytes by TNF-alpha: a case for the neuroprotective role of cytokine. *J Neuroimmune Pharmacol*. 2006; 1:212–22. doi.org/10.1007/s11481-006-9020-8
42. Chiechio S, Copani A, De Petris L, Morales ME, Nicoletti F, Gereau RW 4th. Transcriptional regulation of metabotropic glutamate receptor 2/3 expression by the NF-kappaB pathway in primary dorsal root ganglia neurons: a possible mechanism for the

analgesic effect of L-acetylcarnitine. *Mol Pain*. 2006; 2:20. doi.org/10.1186/1744-8069-2-20

43. Richter M, Suau P, Ponte I. Sequence and analysis of the 5' flanking and 5' untranslated regions of the rat N-methyl-D-aspartate receptor 2A gene. *Gene*. 2002; 295:135–42. doi.org/10.1016/S0378-1119(02)00833-8
44. Begni S, Moraschi S, Bignotti S, Fumagalli F, Rilloi L, Perez J, Gennarelli M. Association between the G1001C polymorphism in the GRIN1 gene promoter region and schizophrenia. *Biol Psychiatry*. 2003; 53:617–19. doi.org/10.1016/S0006-3223(02)01783-3
45. Henley JM, Wilkinson KA. AMPA receptor trafficking and the mechanisms underlying synaptic plasticity and cognitive aging. *Dialogues Clin Neurosci*. 2013; 15:11–27.
46. Zhang G, Li J, Purkayastha S, Tang Y, Zhang H, Yin Y, Li B, Liu G, Cai D. Hypothalamic programming of systemic ageing involving IKK- β , NF- κ B and GnRH. *Nature*. 2013; 497:211–16. doi.org/10.1038/nature12143
47. Bade AN, Zhou B, Epstein AA, Gorantla S, Poluektova LY, Luo J, Gendelman HE, Boska MD, Liu Y. Improved visualization of neuronal injury following glial activation by manganese enhanced MRI. *J Neuroimmune Pharmacol*. 2013; 8:1027–36. doi.org/10.1007/s11481-013-9475-3